# Machine Learning-Aided Indoor Positioning Based on Unified Fingerprints of Wi-Fi and BLE

Shunsuke Tsuchida *, Takumi Takahashi *, Shinsuke Ibi †, and Seiichi Sampei *
*Department of Information and Communications Technology, Osaka University, Yamada-oka 2-1, Suita, 565-0871, Japan
† Faculty of Science and Engineering, Doshisha University, 1-3 Tataramiyakodani, Kyotanabe, 610-0394, Japan
Email: *tsuchida@wcs.comm.eng.osaka-u.ac.jp, {takahashi, sampei}@comm.eng.osaka-u.ac.jp, *sibi@mail.doshisha.ac.jp

***Abstract*—This paper deals with an indoor positioning with the aid of machine learning based on the received signal strength indication (RSSI) fingerprints of beacon signals of both Wi-Fi and Bluetooth low energy (BLE). In fingerprint positioning, a site-survey is conducted in advance to build the radio map which can be used to match radio signatures with specific locations. Thus, it can take the impacts of empirical indoor environments into consideration. However, even if the physical positional relationship in the indoor environment is static, the observed RSSI values are dynamically fluctuated according to the probabilistic wireless channels. Unfortunately, it is difficult to analytically capture the stochastic behavior of RSSI in real-environments, and the accuracy of position estimation is degraded due to the model errors. To tackle this challenging problem, machine learning-based logistic regression is applied to fingerprint positioning with the RSSI data set (available as big data). Additionally, by exploiting a unified fingerprint generated from both Wi-Fi and BLE beacon signals, further performance improvement in the estimation accuracy is possible, owing to the transmit diversity effects. The experimental results show the validity of the proposed positioning scheme with the unified Wi-Fi and BLE fingerprint.**

## I. Introduction

In recent years, mobile high-functional terminals, such as smartphones and tablets, are in widespread use, and geolocation information services are essential for daily life using the mobile terminals. For providing such services to outdoor terminals, global navigation satellite system (GNSS) plays a vital role. However, GNSS cannot show good results when detectors are located in indoor environments, since GNSS requests non-line-of-sight (NLOS) to artificial satellites [1]. In addition to geolocation services on outdoor like map applications, there is also demand on indoor use, for example, advertisement display at the shop front, navigation inside a building, presence confirmation in office, as well as medical and healthcare. Thus, developments of indoor positioning system instead of GNSS is urgent.

To this end, Wi-Fi received signal strength indicator (RSSI)-aided positioning has been actively explored so far [2]–[6]. The indoor positioning of Wi-Fi can be roughly classified into two types: triangular positioning [7] and fingerprint positioning [8]. Unfortunately, the RSSI is not stable due to shadowing and fading phenomena, which induce stochastic problems for the indoor positioning. On the other hand, Bluetooth low energy (BLE), which is often installed in the smartphone, is also useful for positioning. BLE is designed for transmitting small-volume sensing data and text data without sacrificing energy consumption and is expected as a central role for supporting wireless access of IoT (Internet of Things). Thanks to the feature of low power consumption, the mobile terminals shall simultaneously transmit beacon signals of Wi-Fi and BLE for improving the accuracy of the position estimation with the aid of transmit diversity effects.

In this paper, we consider unified fingerprints constituted by both Wi-Fi and BLE beacon signals. Mobile terminals send the beacons to large numbers of receivers settled under the ceiling of a room. Note that the beacons are not radiated from anchor nodes in the room, but done from the mobile terminals. In BLE systems, the receiver suffers from interference in 2.4 GHz industry science medical (ISM) band and noise due to low transmit power signals [9]. In order to avoid the interference, three advertising channels (2402, 2426, and 2480 MHz) are allocated in Wi-Fi channel gaps. By using the advertising channels, the negative impacts of the interference are mitigated. For suppressing the impact of noise, multiple RSSI signals are observed in the receiver. On the other hand, the transmission power of Wi-Fi is much higher than that of BLE, resulting in more accurate RSSI measurement. However, authentication is required before communicating with access point (AP). Without the authentication, service set ID (SSID) beacon signal is available, but the time interval is much longer than that of BLE. Consequently, the estimation accuracy based only on the Wi-Fi beacons is significantly degraded due to lack of the obtained RSSI samples.

The fingerprint approach has two phases: training phase (offline) and testing phase (online). In the training phase, RSSI vectors are captured as training data before the testing phase. In the typical testing phase, maximum likelihood estimation (MLE) is performed by comparing an observed RSSI vector and the fingerprint training data. Unlike triangular positioning on the basis of an optimistic propagation model, the fingerprint positioning can take into account empirical indoor environments. The validity of the fingerprint positioning has been reported in some literature [9]–[13]. They are based on the assumption that the position of the receiver and the beacon transmitter are static. However, even if the location relationship is static, the measured RSSI fluctuates stochastically in indoor wireless channels. Under such circumstance, the testing data differs slightly from training data, resulting in performance degradation in position estimation.

To deal with the above insufficient fingerprint problem, ma-

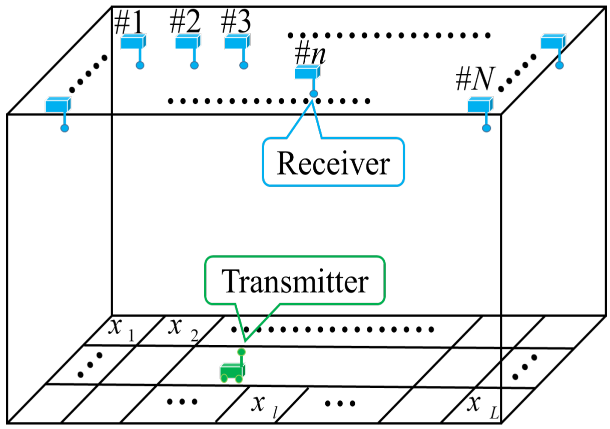


Fig. 1. A structure of the indoor positioning system.

chine learning techniques are applied to the unified fingerprint positioning. Main contributions of this paper are to demonstrate the validity of the unified fingerprint by substantiative experiments with the aid of commercially available Wi-Fi and BLE dongles.

The remainder of this paper is organized as follows. Sect. II presents an indoor positioning model using RSSI, and state a problem to be addressed. In the context of the problem statement, multi-layer perceptron as a machine learning approach is explained in Sect. III. Sect. IV characterizes the validity of the proposed method on the basis of experimental results. Finally, Sect. V concludes the paper with a brief summary.

## II. INDOOR LOCALIZATION USING RSSI

### A. Indoor RSSI measurement

Fig. 1 shows a structure of the indoor wireless environments. A transmitter (TX) on the floor sends beacon signals of both Wi-Fi and BLE to the $N$ receivers (RX) mounted under the ceiling board. BLE assigns 37 ch, 38 ch, and 39 ch for advertising events to send beacon signals. This paper utilizes only 37 ch beacon signal for stabilizing frequency selective fading behavior. On the other hand, Wi-Fi exploits 1 ch of IEEE 802.11g. The floor is segmented into $L$ square cells, where the $l$-th cell is denoted by $x_l$. For ease of the analysis, we assume that the TX is placed at the center of each cell $x_l$. Time intervals of beacon transmission of Wi-Fi and BLE are denoted by $T_{\rm W}$ and $T_{\rm B}$ [sec], respectively.

Each RX yields the RSSI vector $\boldsymbol{y} = [\boldsymbol{y}_{\rm W}^{\rm T}, \boldsymbol{y}_{\rm B}^{\rm T}]^{\rm T}$ at intervals of $T_{\rm R}$ [sec], where $\boldsymbol{y}_i = [y_W(1), y_W(2), \ldots, y_W(N), y_B(1), y_B(2), \ldots, y_B(N)]^{\rm T}$ resulting in $2N$ elements in $\boldsymbol{y}$ . Note that $(\cdot)^{\rm T}$ indicates the transpose of the vector. $\boldsymbol{y}_i(n)(i \in W, B)$ is an averaged value over raw RSSI obtained from the $n$-th RX during $T_{\rm R}$. Each RX notifies $y_i(n)(i \in W, B)$ to a fusion center by using Wi-Fi network for forming the RSSI vector $\boldsymbol{y}$.

### B. Fingerprint Positioning

In the training phase, the fusion center monitors RSSI vector $\boldsymbol{y}$ while transmitting beacon from each cell $x_l$. The training vector $\boldsymbol{t}_l$ is constructed by averaging the observed RSSI vector in the time domain, where the average interval should be set to longer than the transmission interval.

In the testing phase, as a typical approach, MLE finds the most likely position $x_l$ of TX on the basis of Euclidean distance, which is given by

$$\hat{x}_l = \arg\max_{x_l} |\boldsymbol{y} - \boldsymbol{t}_l|. \tag{1}$$

In the typical fingerprint positioning described above, the accuracy can be higher than triangular positioning because it is experimentally measuring RSSI. This method assumes that RSSI is uniquely determined between arbitrary TX and RX. However, the actual RSSI stochastically fluctuates even if TX does not move. Under such circumstance, the testing data slightly differs from training data even though the positions of TX and RX are the same, resulting in performance degradation. To deal with this problem, neural-network aided positioning is applied in the next section.

## III. MULTI-LAYER PERCEPTION-AIDED POSITIONING

### A. Multi-class classification model

The simplest neural network model in machine learning based on logistic regression is simple perceptron, which can classify the test data into two classes. As an activation function, a step function is utilized. On the other hand, for indoor positioning, it is necessary to classify the data into more classes. Such a multiple class classification becomes possible by replacing the step function with a softmax function for yielding quasi-probability, something like belief.

For the input of the $K$-dimensional vector $\boldsymbol{z} = [z_1, \ldots, z_k, \ldots, z_K]^{\rm T}$ the softmax function is expressed as

$$f(\boldsymbol{z}) = \frac{\mathrm{e}^{\boldsymbol{z}}}{\sum_{k=1}^{K} \mathrm{e}^{z_k}}. \tag{2}$$

Using (2), multi-class classification for the unified fingerprint positioning is performed by

$$\tilde{\boldsymbol{x}} = f(\boldsymbol{W}\boldsymbol{y} + \boldsymbol{b}), \tag{3}$$

where $\boldsymbol{W}$ represents a matrix of size $L \times 2N$, and the element in the $l$-th row and $k$-th column is weight of RSSI observed at input $\#k$ at candidate $x_l$. The column vector $\boldsymbol{b}$ of size $L$ is a bias. This model is referred to as multinomial logistic regression. Here, the appropriate weight matrix $\boldsymbol{W}$ and bias vector $\boldsymbol{b}$ are computed (learned) from training data $\boldsymbol{t}_l$ in advance to construct the resultant neural network. Finally, the index $l$ corresponding to the highest value (quasi-probability) in $\tilde{\boldsymbol{x}}$ indicates the most likely position $x_l$.

### B. Multi-layer perceptron

In principle, positioning is a nonlinear regression problem. Therefore, multi-layer perceptron (MLP) should be utilized as the neural network for the multi-class classification, which consists of input, hidden, and output layers. Here, the output of the hidden layer is expressed as

$$\boldsymbol{h} = g(\boldsymbol{U}\boldsymbol{y} + \boldsymbol{c}). \tag{4}$$

where $g(\boldsymbol{z})$ is an activation function for the hidden layer. $\boldsymbol{U}$ is a $J \times 2N$ weight matrix and $\boldsymbol{c}$ is a $J \times 1$ bias vector, where $J$

is the number of neurons in the hidden layer. Eextensionally, multiple (4) is serially concatenated to create 3 hidden layers in this paper.

With the aid of the intermediate output $\boldsymbol{h}$, the output of the output layer is given by

$$\tilde{\boldsymbol{x}} = f(\boldsymbol{V}\boldsymbol{h} + \boldsymbol{d}) \tag{5}$$

where weight $\boldsymbol{V}$ is a $L \times J$ weight matrix and $\boldsymbol{d}$ is a $L \times 1$ bias vector.

In MLP, the vanishing gradient problem [14] is a difficult found in gradient-based learning process, resulting in the insufficient model updates. To deal with the problem, we utilize the rectified linear unit (ReLU) function as the activation function in the input and hidden layer. ReLU function is also referred to as the ramp function, and is expressed by

$$g(z_k) = \max(0, z_k). \tag{6}$$

Differentiating (6), we have

$$\frac{dg(z_k)}{dz_k} = \begin{cases} 1 & (z_k > 0) \\ 0 & (z_k \leq 0) \end{cases}. \tag{7}$$

From (7), ReLU function has no curve part and the derivative returns 1 regardless of the value of $z$ when $z$ is non-negative. By using this activation function during the learning, it is possible to prevent the vanishing gradient problem and realize fast model updates [14].

### C. Mini-batch gradient decent

One of the most severe issues in the context of training neural networks using gradient descent method is the time cost for the learning process toward model convergence. As the number of data $D$ increases, the required memory and computational cost for model updates rapidly increase. To avoid the inconvenience, stochastic gradient descent (SGD) is effective [15]. While the typical gradient descent method updates the model parameters after taking the sum of all data, SGD chooses data at random in a set of $D$ data and updates the parameters every instance. Consequently, the model parameters can be updated $D$ times at the same computational cost required for updating the whole parameters once. However, if the parameters are updated after processing every instance, the model update would be too noisy and the process is no longer computationally efficient. As an effective solution taking into account the trade-off between fast model update and memory efficiency, we utilize mini-batch gradient descent method, where the data is divided into $d(\leq D)$ chunks [16].

### D. Dropout

Another challenging problem in MLP learning is over-fitting. To avoid over-fitting, an ensemble of neural networks with different models is effective, however, it requires the additional computational cost for training [17]. As a computationally cheap and effective alternative method, dropout is well known, where the neurons in the neural network are probabilistically dropped out during training. Consequently, we can simulate having a large number of different network architectures using a single model without any additional cost.


Fig. 2. A structure of the indoor positioning system.

TABLE I
EXPERIMENTAL PARAMETERS.

| | |
|---|---|
| Number of cells $L$ | 18 |
| Number of receivers | 8 |
| cell size | $1 \times 1$ $[m^2]$ |
| Wi-Fi Beacon interval $T_{\mathrm{W}}$ | 3 [sec] |
| BLE Beacon interval $T_{\mathrm{B}}$ | 0.3 [sec] |
| Training phase | 24 [hour] |
| Testing phase | 4 [hour] |
| Number of hidden layers | 3 |

## IV. EXPERIMENTAL RESULTS

To confirm the validity of the proposed unified fingerprint positioning, experiments have been conducted in the actual environments. The cell structure is shown in Fig. 2. There are 18 cells with a size of 1 $\times$1 $m^2$ on the floor. Besides, experimental parameters are summarized in Tab. I. BLE beacon transmitter (BLE adapter: BSBT4D09BK) and Wi-Fi beacon transmitter (Buffalo Wi-Fi adapter: WLI-UC-GNM2) are mounted on LEGO Mindstorms EV3. EV3 linearly walks at a speed of 10 [cm/sec] until reaching the edge of the area, and when EV3 reaches the edge, it randomly turns in some other direction. The Wi-Fi and BLE beacon intervals $T_{\mathrm{W}}$ and $T_{\mathrm{B}}$ are 3 [sec] and 0.3 [sec], respectively. Note that Wi-Fi beacon cannot send frequently and the receivers sometimes fail to receive Wi-Fi beacon signal. There are eight receivers under the ceiling board. Wi-Fi beacon receiver (Buffalo Wi-Fi adapter: WLI-UC-GNM2) and BLE beacon receiver (Buffalo BLE adapter: BSBT4D09BK) are mounted on Raspberry Pi 3. In the training phase, EV3 walks in 24 [hour], resulting in 38,000 RSSI observation samples for training data. The camera equipped on the each Raspberry Pi 3 is utilized for capturing

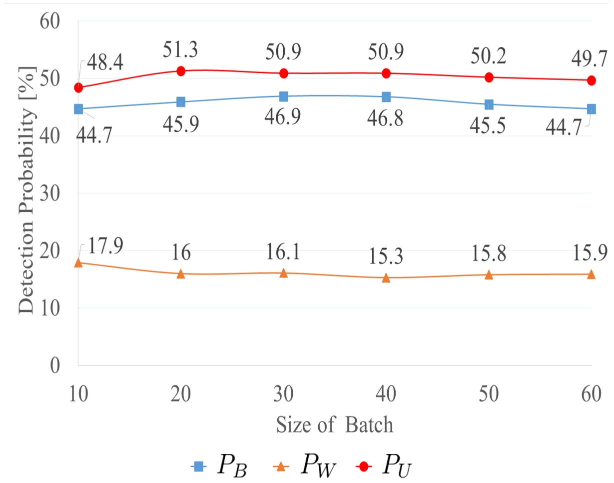


Fig. 3. Probability of $P_{\mathrm{B}}$, $P_{\mathrm{W}}$, and $P_{\mathrm{U}}$ [%] according to Size of Batch.

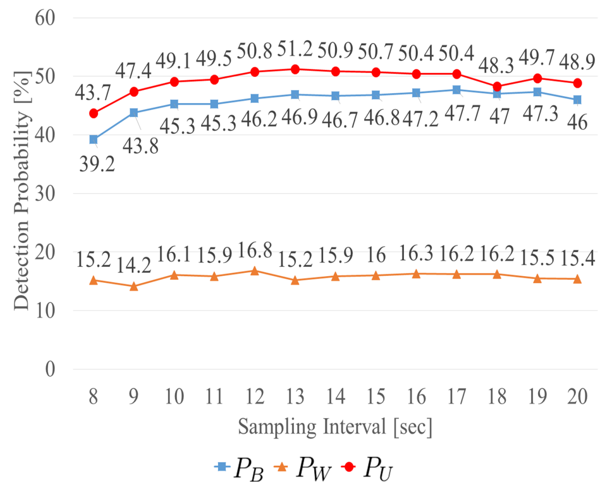


Fig. 5. Probability of sampling interval of $P_{\mathrm{B}}$, $P_{\mathrm{W}}$, and $P_{\mathrm{U}}$ [%].

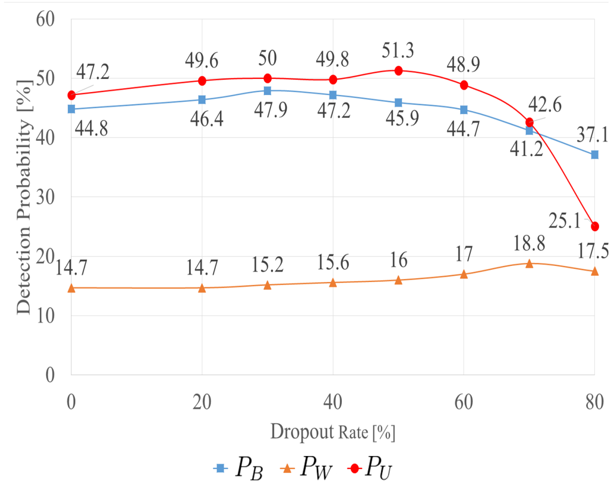


Fig. 4. Probability of $P_{\mathrm{B}}$, $P_{\mathrm{W}}$, and $P_{\mathrm{U}}$ [%] according to Dropout Rate.

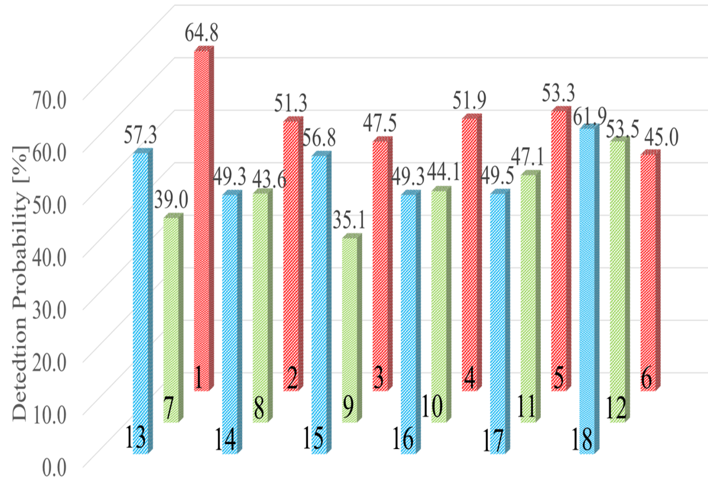


Fig. 6. Probability of detection $P_{\mathrm{U}}$ [%] of unified fingerprint positioning in each cell $x_1 - x_{18}$.

the correct positions for training data. In the testing phase, EV3 walks in 4 [hour], resulting in 6,500 RSSI observation samples for testing data.

Figs. 3, 4, and 5 show the results of the correct detection probability $P_i,\ i \in \{\mathrm{B}, \mathrm{W}, \mathrm{U}\}$. $P_{\mathrm{B}}$ is the probability of BLE, $P_{\mathrm{W}}$ is Wi-Fi, and $P_{\mathrm{U}}$ is the probability of unified Wi-Fi and BLE. Each probability is defined by

$$P_i = \frac{\text{Num. of correctly detected samples}}{\text{Num. of all samples}}. \tag{8}$$

Note that $P_i = 1/18 = 5.6\%$ is the worst case. The default parameters for MLP are as follows:

- Learning rate: $\eta = 0.0008$
- Num. of nodes of input and hidden layer: $J = 550$
- Learning weight in input layer: 0.06
- Learning weight in the first hidden layer: 0.006
- Learning weight in the second hidden layer: 0.00009
- Learning weight in the third hidden layer: 12

The above parameters are tuned to achieve better performance through several positioning trials.

Fig. 3 shows the detection probability when the batch size is changed from 10 to 60. The dropout rate is fixed at 50%. In this case, the optimal size of batch is 20. Fig. 4 shows the correct detection probability when the dropout rate is changed. The batch size is fixed at 20. $P_{\mathrm{W}}$ is not accurate in any case. $P_{\mathrm{B}}$ shows the best accuracy with a value of around 0.7. However, it cannot exceed the best result of $P_{\mathrm{U}}$. Fig. 5 shows the probability of each sampling interval. In this data, the batch size is set to 20 and the dropout rate is 50%. For both $P_{\mathrm{B}}$ and $P_{\mathrm{U}}$, the estimation accuracy achieves the best performance when the sampling interval is around 13 seconds. We can also confirm that the accuracy is very low even if sampling interval is longer or shorter. Unfortunately, $P_{\mathrm{W}}$ is always bad regardless of sampling interval.

Low detection accuracy of Wi-Fi-based estimation is caused by the fact that Wi-Fi beacon signals cannot be obtained at the receivers in a shorter transmission interval compared to BLE beacons. As mentioned before, the authentication is not conducted in this experiment. Thus, any data link from the Wi-Fi AP is not connected to each receiver. Therefore, the receivers have to scan Wi-Fi beacons repeatedly for searching the AP, and it takes a lot of time. The difference in the transmission interval of BLE and Wi-Fi causes deviation in observation data and affects the estimation accuracy.

As can be seen from the table results, $P_{\mathrm{U}}$ shows better results than $P_{\mathrm{B}}$ or $P_{\mathrm{W}}$. Figs. 3, 4, and 5 explicitly demonstrate the unification of BLE and Wi-Fi is effective.

In Fig. 6, the detection probability $P_{\mathrm{U}}$ of unified fingerprint positioning in each cell $x_l$ is characterized. As you can see from this figure, the estimation accuracy tends to be lower at the arbitrary candidate point in the middle of the room because the feature extraction is difficult in the fingerprint-based learning. Consequently, the detection errors to adjacent candidate points frequently occur. Similarly, the candidate points at the corner, for example $x_1$, $x_6$, $x_{13}$, and $x_{18}$, have similar characteristics. However, the probability of $x_6$ is extremely bad among them. As you can see from Fig. 2, $x_6$ is close to furniture. There is a possibility that the disturbance of the radio wave by the furniture is affecting.

## V. CONCLUSION

In this paper, we proposed an indoor positioning with the aid of machine learning based on MLP using unified RSSI fingerprints generated from both Wi-Fi and BLE beacon signals. The validity of the proposed positioning scheme was demonstrated by experiments in the actual environment using commercially available Wi-Fi and BLE dongles. In any batch size, dropout rate, and sampling interval, the correct detection probability based on the unified RSSI fingerprints $P_{\mathrm{U}}$ achieves better performances compared to $P_{\mathrm{B}}$ and $P_{\mathrm{W}}$. More specifically, $P_{\mathrm{U}}$ is $5\%$ better than $P_{\mathrm{B}}$ owing to the transmit diversity effects. However, there still remains room for improvement in the position detection accuracy, for example, we have to take into account the spatial correlation among the observed RSSI vectors. Additionally, we are also considering a neural network model and activation function more suitable for fingerprint-based positioning. Furthermore, we are planning to utilize different channels of Wi-Fi and BLE to improve the versatility of RSSI data. These works are still left for the future work.

## ACKNOWLEDGEMENT

A part of this work was financially supported by JSPS KAKENHI Grant Number 16K06354, Japan.

## REFERENCES

[1] S. Schon and O. Bielenberg, "On the capability of high sensitivity gps for precise indoor positioning," in *2008 5th Workshop on Positioning, Navigation and Communication*, March 2008, pp. 121–127.

[2] D. Dardari, P. Closas, and P. M. Djuri, "Indoor tracking: Theory, methods, and technologies," *IEEE Transactions on Vehicular Technology*, vol. 64, no. 4, pp. 1263–1278, April 2015.

[3] M. E. Rusli, M. Ali, N. Jamil, and M. M. Din, "An improved indoor positioning algorithm based on rssi-trilateration technique for internet of things (iot)," in *2016 International Conference on Computer and Communication Engineering (ICCCE)*, July 2016, pp. 72–77.

[4] W. W. Li, R. A. Iltis, and M. Z. Win, "A smartphone localization algorithm using rssi and inertial sensor measurement fusion," in *2013 IEEE Global Communications Conference (GLOBECOM)*, Dec 2013, pp. 3335–3340.

[5] Y. Li, J. Chen, Y. Shi, Y. Cheng, and L. Wang, "Wifi-assisted multi-floor indoor localization with inertial sensors," in *2016 8th International Conference on Wireless Communications Signal Processing (WCSP)*, Oct 2016, pp. 1–5.

[6] S. P. Khare, J. Sallai, A. Dubey, and A. Gokhale, "Short paper: Towards low-cost indoor localization using edge computing resources," in *2017 IEEE 20th International Symposium on Real-Time Distributed Computing (ISORC)*, May 2017, pp. 28–31.

[7] A. Thaljaoui, T. Val, N. Nasri, and D. Brulin, "Ble localization using rssi measurements and iringla," in *2015 IEEE International Conference on Industrial Technology (ICIT)*, March 2015, pp. 2178–2183.

[8] M. Ohtani, H. Iwai, and H. Sasaoka, "Improvement of position estimation accuracy using multiple access points in terminal position estimation based on position fingerprint," in *2014 International Symposium on Antennas and Propagation Conference Proceedings*, Dec 2014, pp. 399–400.

[9] S. Silva, S. Soares, T. Fernandes, A. Valente, and A. Moreira, "Coexistence and interference tests on a bluetooth low energy front-end," in *2014 Science and Information Conference*, Aug 2014, pp. 1014–1018.

[10] S. Alraih, A. Alhammadi, I. Shayea, and A. M. Al-Samman, "Improving accuracy in indoor localization system using fingerprinting technique," in *2017 International Conference on Information and Communication Technology Convergence (ICTC)*, Oct 2017, pp. 274–277.

[11] N. Alikhani, S. Amirinanloo, V. Moghtadaiee, and S. A. Ghorashi, "Fast fingerprinting based indoor localization by wi-fi signals," in *2017 7th International Conference on Computer and Knowledge Engineering (ICCKE)*, Oct 2017, pp. 241–246.

[12] A. Nikitin, C. Laoudias, G. Chatzimilioudis, P. Karras, and D. Zeinalipour-Yazti, "Indoor localization accuracy estimation from fingerprint data," in *2017 18th IEEE International Conference on Mobile Data Management (MDM)*, May 2017, pp. 196–205.

[13] X. Tian, R. Shen, D. Liu, Y. Wen, and X. Wang, "Performance analysis of rss fingerprinting based indoor localization," *IEEE Transactions on Mobile Computing*, vol. 16, no. 10, pp. 2847–2861, Oct 2017.

[14] A. Krizhevsky, I. Sutskever, and G. E. Hinton, "Imagenet classification with deep convolutional neural networks," in *Advances in neural information processing systems*, 2012, pp. 1097–1105.

[15] L. Bottou and O. Bousquet, "The tradeoffs of large scale learning," in *Advances in Neural Information Processing Systems 20 (NIPS 2007)*, J. Platt, D. Koller, Y. Singer, and S. Roweis, Eds. NIPS Foundation, 2008, pp. 161–168.

[16] L. Bottou, "Online algorithms and stochastic approximations," in *Online Learning and Neural Networks*, D. Saad, Ed. Cambridge, UK: Cambridge University Press, 1998, revised, oct 2012.

[17] N. Srivastava, G. Hinton, A. Krizhevsky, I. Sutskever, and R. Salakhutdinov, "Dropout: a simple way to prevent neural networks from overfitting," *The Journal of Machine Learning Research*, vol. 15, no. 1, pp. 1929–1958, 2014.